Available online at www.sciencedirect.com

ScienceDirect

Energy Procedia 43 (2013) 44 – 53

Energy Procedia

4th Workshop on Metallization for Crystalline Silicon Solar Cells

Replacement of silver in silicon solar cell metallization pastes containing a highly reactive glass frit: Is it possible?

Dominik Rudolph[1*], Sara Olibet[1], Jaap Hoornstra[2], Arthur Weeber[2], Enrique Cabrera[1], Anna Carr[2], Martien Koppes[2], Radovan Kopecek[1]

[1]*International Solar Energy Research Center – ISC Konstanz, Rudolf Diesel-Str. 15, D-78467 Konstanz, Germany*
[2]*ECN Solar Energy, Westerduinweg 3, NL-1755 LE Petten, the Netherlands*
**Email: dominik.rudolph@isc-konstanz.de*

Abstract

Massive savings in silicon solar cell production could be achieved by replacing the costly Ag in front side metallization pastes against cheaper metals like Ni or Zn. Regarding the attempt to split the metallization process up into a two step process, first printing a paste containing Ni or Zn instead of Ag for contact formation and second printing a conducting paste containing e.g. Cu, this work is restricted to the investigation of the contacting paste. Simple pastes containing only Ni or Zn respectively, rudimentary glass frit, organic binder and solvent were tested on wafers with a low resistivity emitter using various fast firing profiles and annealing. Our first attempts using Ag compatible frits have shown that it is possible to create a contact to Si yet it is significantly worse than with comparable silver pastes. SEM measurements of the contact area after selective metal/glass etch have shown a strong Si etching by the investigated pastes and only insufficient crystallite formation. This explains the reduced open circuit voltage, pseudo fill factor and the high contact resistivity measured on the cells. Our investigations show that it is very hard to exchange Ag by another metal without fundamentally changing the paste formulation and/or the firing conditions.

Selection and peer-review under responsibility of Guy Beaucarne, Gunnar Schubert and Jaap Hoornstra

Keywords: silver replacement; silicon solar cell; screen printing paste; nickel; zinc; contact formation;

1. Introduction

Approximately 30% of the non base material related costs of a crystalline silicon solar cell are contributed by the silver in the screen printing paste [1]. In the last years the price of Ag was drastically increasing, which is due to more need of Ag in the electronics industry and money investments into Ag due to the financial crisis. Savings in Ag paste are therefore essential for the photovoltaic industry. First steps are already realized by the reduction of

Selection and peer-review under responsibility of Guy Beaucarne, Gunnar Schubert and Jaap Hoornstra
doi:10.1016/j.egypro.2013.11.087

the amount of Ag in the front grid and rear side pad pastes and of the amount of printed paste by printing finer lines, which is limited by the screen printing technology. Also printing of a thin Ag seed layer with subsequent Ag plating improves the line conductivity of the fingers in comparison to conventional screen printed Ag fingers, decreasing the amount of Ag required. However, the most desirable approach is to substitute Ag completely. Some groups are working on a printable low temperature sintering copper paste for application to ITO in Si heterojunction solar cells [2]. Cu plating on a seed layer is another promising approach, where the thin seed layer could be produced by aerosol printing, plating or excimer laser treatment of e.g. nickel with pre opening of the SiN_x antireflection layer [3, 4].

The aim of this work was to create test firing-through pastes containing different metals together with simplest glass frit using the results as input for simulation systems which could describe the dynamic contact formation and the static current transport [5, 6]. To simplify the system we focused on splitting up the current Ag-based pastes bi-functionality of forming good contact to Si and simultaneously transporting the collected current in highly conductive lines within a double screen-print approach. Thus we print a paste, which enables the contact formation to Si in a first step and only requires a second printing/drying step of low-temperature Cu paste for line conductivity.

Two metals were chosen as alternative contacting material: nickel and zinc. Ni is cheap and can make a good contact to Si by means of Ni silicides [7]. One disadvantage of Ni is its fast interstitial diffusion in Si at elevated temperatures. Interstitial nickel ions are even mobile in Si at room temperature [8]. Also zinc could be a possible material to substitute Ag because of its low cost and similar properties. Both metals have a higher specific electrical resistivity than silver: $\rho_{Ni} = 8.7\ \mu\Omega$ cm and $\rho_{Zn} = 6.1\ \mu\Omega$ cm as compared to $\rho_{Ag} = 1.6\ \mu\Omega$ cm [9], which makes it necessary to increase the line conductivity of the fingers in a second printing step for example by Cu paste. In this regard Ni has an advantage over Zn because it serves as diffusion barrier for Cu while for Zn no such properties are known. Ni and Zn pastes were tested in comparison with an Ag paste containing the same simple glass frit. The cells were fired under various conditions in a fast firing furnace and also sintering at lower temperature was applied on the cells printed with Ni and Zn paste.

2. Sample processing and experimental setup

Monocrystalline silicon samples were prepared for the experiments. After texturization with KOH the Cz-Si wafers were cleaned in HCl and HF baths. A strong 50 Ω/sq $POCl_3$ diffusion was used for emitter formation to enable a good contact formation with the used rudimentary metallization pastes. After diffusion and phosphorus glass etching the front surface was passivated by a SiN_x antireflection layer. A part of the samples was left unpassivated to examine the functionality of the pastes on both surfaces.

Three different pastes, which are listed in Table 1, were made using the same simple glass frit, organic binder and solvent.

Table 1: Experimental matrix and composition of the glass frit.

		Composition of the glass frit		
paste	metal in mass%	PbO in mass%	B_2O_3 in mass%	SiO_2 in mass%
1	Ag 76%			
2	Ni 69%	86	11	3
3	Zn 65%			

These pastes were printed on the cells with a screen containing 120 µm finger openings. On the rear side full surface aluminum metallization was performed. Fast firing was applied varying peak-temperature, time at temperature, temperature ramp-up and also firing atmosphere. For some samples firing of the wafers with Al rear side was done before printing of the Ni and Zn pastes to achieve a good back surface field while annealing the

front side metallization afterwards at low temperature. Characterization includes IV measurements, Suns-V_{oc} measurements, contact resistivity measurements and SEM pictures made after different selective contact etching steps. In addition, EDX measurements on cross section SEM pictures were made.

3. Results

3.1. Results with silver pastes

An Ag paste based on the same glass served as reference for the non-Ag pastes. Results of the tested various fast firing temperature settings are shown in Fig. 1. As expected the results with this simple paste composition were not as good as the commercially available state of the art silver pastes, but satisfying. As the low pseudo fill factors (pFF) indicate, the open circuit voltages are strongly reduced due to emitter damage. This effect is stronger with higher firing temperature and longer dwell time as Fig. 1 shows. The high contact resistances at low firing temperatures are responsible for the low fill factors (FF). At high temperatures or moderate temperatures with long dwell time the contact resistivity is lower but the FF is limited through the pFF by emitter damage.

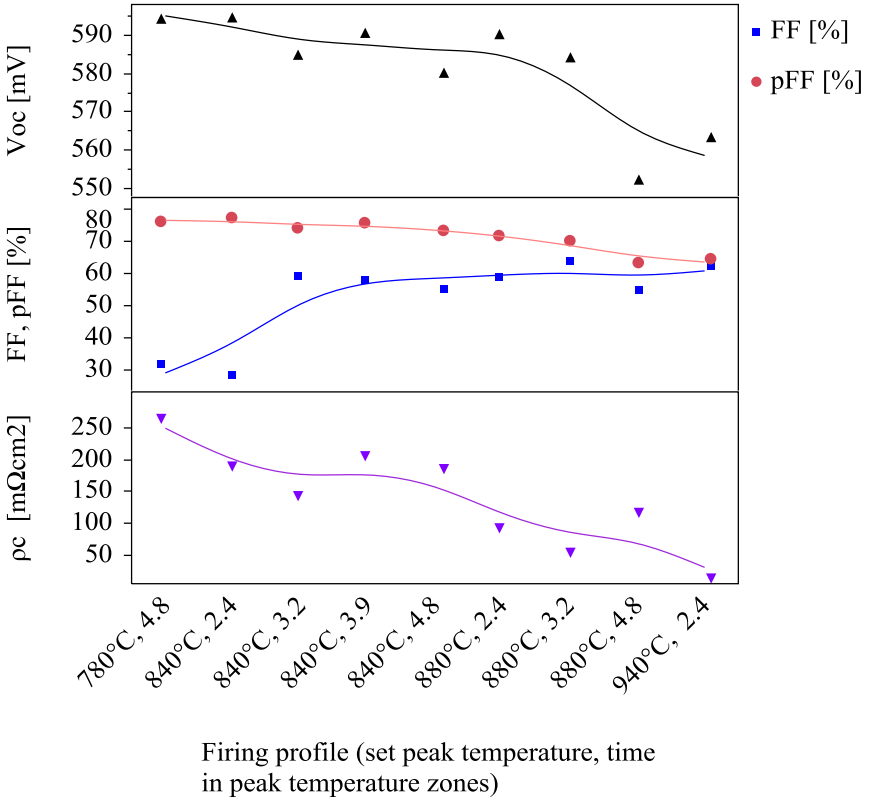

Fig. 1: V_{oc}, FF, pFF and ρ_C versus the fast firing temperature profile used for Ag paste sample firing.

SEM pictures were made after selective metal and glass etch of the fingers. Figure 2 a) shows an Ag paste sample fired for 4.8 s at T_{peak} = 780°C after selective silver etch. The Si surface is covered by a thick glass layer containing precipitates. After full etch of the silver contact it can be observed that at these low temperatures the Si is strongly etched by our paste see Fig. 2 b). There are only very few small Ag crystallite imprints visible, which explains the high contact resistivity of around 250 mΩcm^2. Fig. 3 shows the selective metal and glass etch as well as the full etch of an Ag sample fired for 2.4 s at T_{peak} = 960°C. Selective metal and glass etch exposes crystallites

and precipitates, which lay underneath the glass layer, on the surface, see Fig. 3 a). Nearly the whole surface is coated with metal crystallites and precipitates. The full etch of the sample shows many large imprints of various shapes of etched away Ag crystallites, as indicated in Fig. 3 b). This explains the lower contact resistivity of 23 $m\Omega cm^2$ and hence the higher FF and J_{sc} compared to the sample fired at 780°C, see again Fig. 1. The strong etching of the Si surface and the deep imprints are responsible for the reduced pFF and V_{oc}.

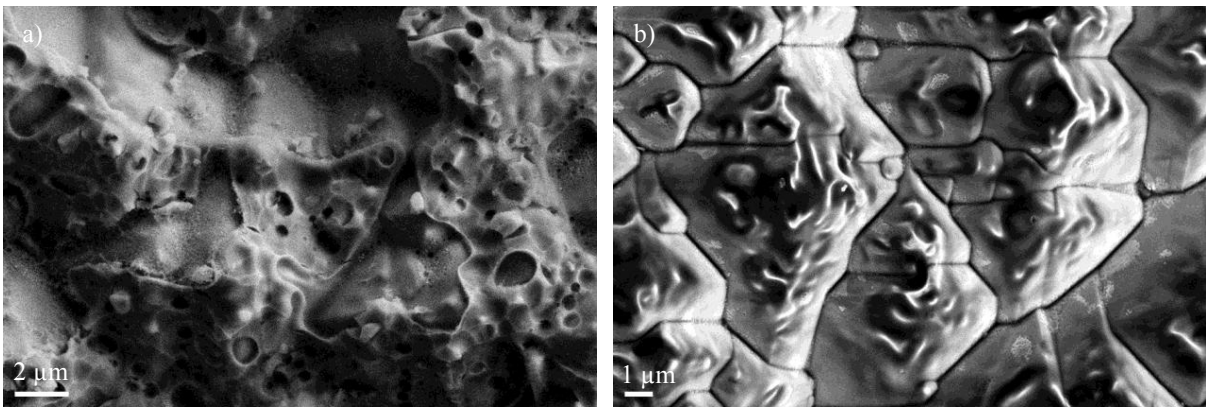

Fig. 2: SEM micrographs after a) selective metal (Ag) etch and b) full contact etch. These samples were fired for 4.8 s at T_{peak} = 780°C.

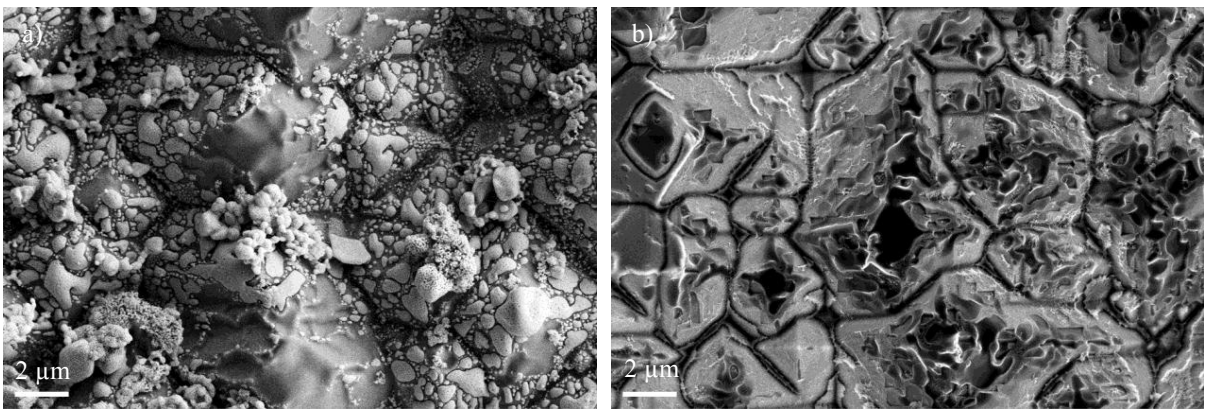

Fig. 3: SEM micrographs after a) selective metal and glass etch and b) full contact etch. These samples were fired for 2.4 s at T_{peak} = 960°C.

3.2. Results with nickel pastes

Despite the large temperature/time parameter space tested, neither by fast firing nor by tempering a good contact to Si could be formed, because sufficient Ni silicide formation could not be achieved. The microscopic interfaces resulting from high temperature fast-firing show Si/Pb crystallites with small Ni content grown into Si, see Fig. 4 and Table 2. Equally which kind of firing was used the adhesion of the paste was such poor that most of the Ni bulk dropped off after firing.

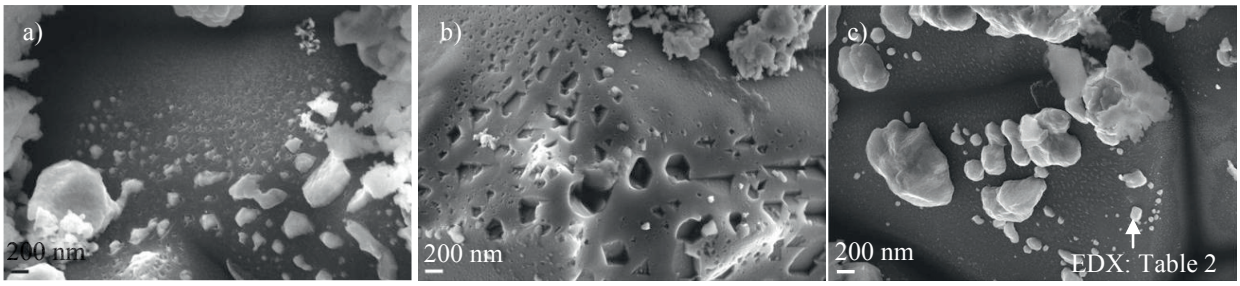

Fig. 4: SEM micrographs after a) selective metal (Ni) and glass etch, b) full contact etch and c) selective metal (Ni) and glass etch with EDX measurement area of a sample fired at 960°C for 3.8 s. The density of crystallites is very high but they are consisting of Pb and Si with a small Ni content only.

Table 2: EDX measurement results from the point highlighted in Fig. 4 c).

element	mass%	standard deviation mass%
C K	6.14	1.78
O K	5.11	0.89
Si K	37.74	1.53
Ni L	3.52	1.04
Pb M	47.49	1.96

Due to the strong etching of the Si surface and the large crystallites pFF and V_{oc} are decreased, affected strongly by the firing temperature, as shown in Fig. 5. The FF is low for the samples without SiN at low firing temperatures and is not measurable anymore with increasing firing temperature. For the samples with SiN it is not measurable over the whole tested firing temperature range.

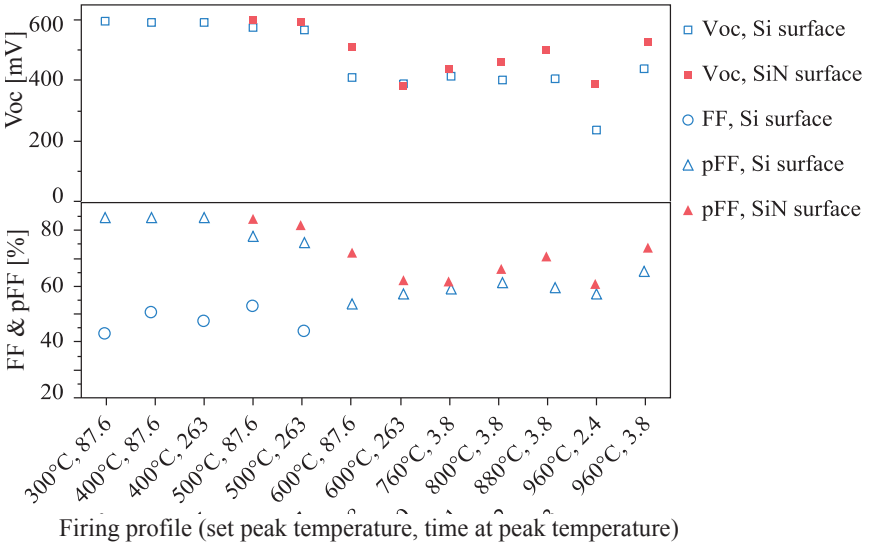

Fig. 5: V_{oc}, FF and pFF of the Ni samples fired at different firing profiles.

Full etch pictures of samples tempered at low temperatures are shown in Fig. 6 a) and b). At 400°C there are many small imprints without any visible etching damage to the Si from the glass. The corresponding crystallites are quite small and most likely they lay underneath the glass layer. At 500°C the imprints are obviously larger and reach further into the silicon. V_{OC} and pFF are strongly decreased, which shows that in addition the emitter is damaged by in-diffusion of foreign atoms. The high contact resistivity shows that the contact area between Ni silicides and Si is too small or the silicides are separated through the glass layer from the Ni bulk. The cross section SEM of a finger verifies this assumption, see Fig. 6 c). There are some small crystallites inside the Si and above is a thick glass layer. EDX measurement results of the crystallite highlighted in Fig. 6 c) are summarized in Table 3. Besides nickel, silicon and lead are detected. Therefore it is hard to say which kind of nickel silicides are formed or if the Pb content in the crystallite is indeed as large as measured. However, the main problem of the tested Ni paste is its poor adhesion.

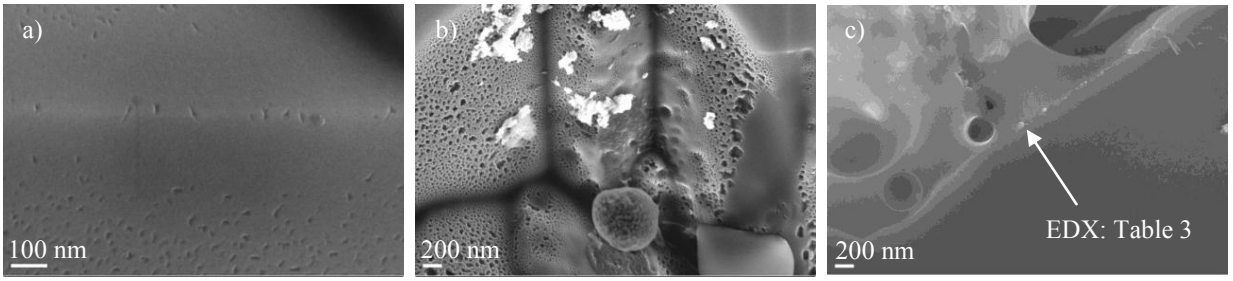

Fig. 6: SEM micrographs after full etch of the Nickel-paste contacts after 90 s tempering a) at 400°C and b) at 500°C. c) SEM micrograph of a cross section Si wafer printed with Ni paste and tempered for 90 s at 500°C including EDX spot measurement of a crystallite.

Table 3: EDX measurement results from crystallite in Fig. 6 c).

element	mass%	standard deviation mass%
O K	3.82	0.56
Si K	53.24	0.71
Ni L	5.91	0.35
Pb M	37.03	0.74

3.3. Results with zinc pastes

After firing of the zinc samples under air atmosphere the metal fingers have such a poor adhesion, that the metal could be abraded with a wipe. This indicates that either no sufficient sintering between the zinc particles takes place during the fast firing process in ambient air or the anchorage between the Si and the metal finger is weak. This poor adhesion was not seen under N_2 firing atmosphere, which means that some kind of side reaction between the Zn particles and the air atmosphere handicaps the sintering. IV and Suns-V_{OC} results of the zinc paste printed on Si and SiN samples and fired with different profiles are shown in Fig. 7. The V_{oc} of the SiN as well as of the Si samples is high at low temperatures without any relevance of the time at peak temperature, and decreases with increasing firing temperature. The same observation is made for the pseudo fill factor. This indicates a strong Si etching dependence on temperature as we have seen with the silver paste. The fill factor is not measurable at firing temperatures up to 700°C and at 960°C. The maximum FF is reached at 720°C and with increasing firing temperature the fill factor and the pFF gradually decrease.

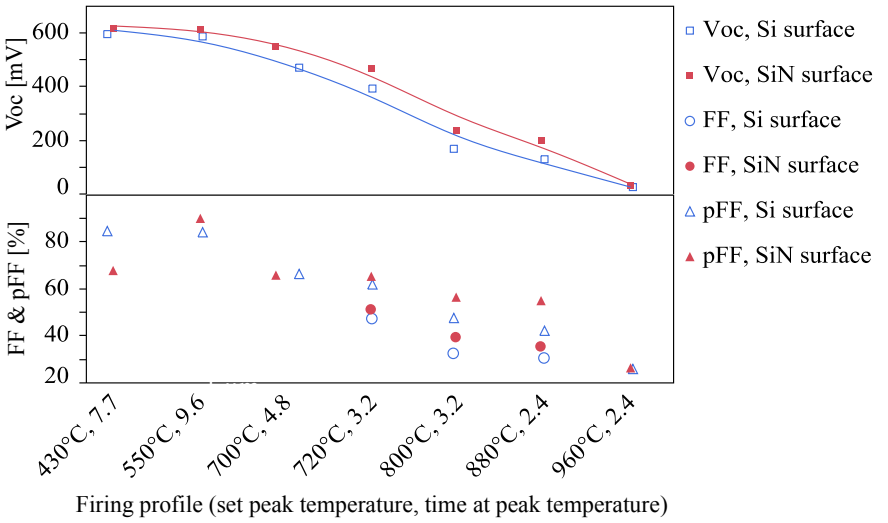

Fig. 7: V_{oc}, FF and pFF of the zinc paste samples fired at different firing profiles with and without SiN surface passivation.

Figure 8 a) and b) show SEM pictures after full metal and glass etch of samples with SiN fired at low (550°C) and at high peak firing temperature (960°C). In Fig. 8 a) the surface is slightly etched and no imprints are visible, while in Fig. 8 b) the Si surface is strongly etched and many large imprints are visible. This is one explanation of the drop in pFF and Voc with increasing firing temperature. But if we compare Fig. 8 b) with the Ag sample at 960°C (Fig. 3 c)) we see that the Si etching and the imprints are comparable, which means that this is not the only source for the strong V_{oc} and pFF reduction of the Zn samples.

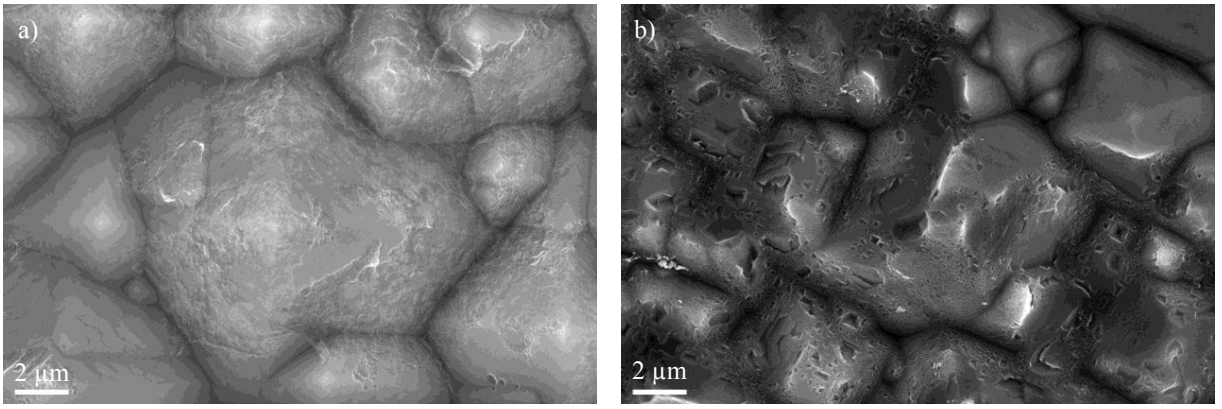

Fig. 8: SEM pictures of full etched SiN samples printed with the Zn paste. The difference between low firing temperature 560°C, a) and high firing temperature 960°C, b) is clearly visible. With higher temperature the Si is etched stronger and more imprints are formed.

Cross sections of fired Si samples printed with Zn paste show crystallites see Fig. 9. EDX measurement results of one of these crystallites are summarized in Table 4. The high Pb content in the crystallites could be one explanation for the high contact resistivity and hence the bad series resistance.

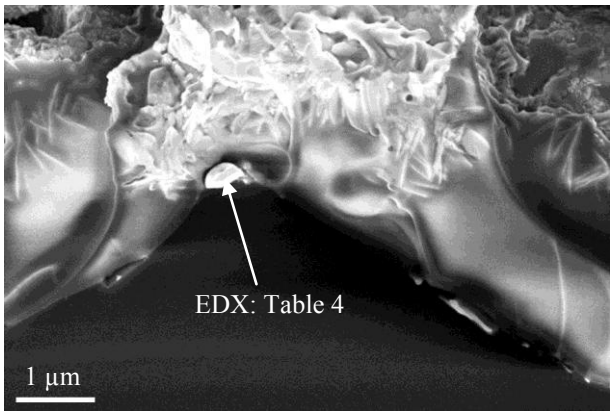

Fig. 9: Cross section of a Si sample printed with Zn paste and fired under air at 880°C peak temperature.

Table 4: Results of the EDX measurement of the Zn paste crystallite in the middle of Fig. 9.

element	mass%	standard deviation mass%
C K	5.09	1.12
O K	7.40	1.20
Si K	3.29	0.84
Zn L	10.96	1.62
Pb M	73.27	2.87

4. Discussion

4.1. Nickel

The reduction of pFF to around 60 - 70% and V_{oc} to around 400 – 500 mV is not only explainable by the emitter etching and the large crystallites, which reach deep inside the emitter, see Fig. 4 b). The etching and the crystallite size are comparable with the one resulting from the silver paste in Fig. 3 b). For the silver paste the pFF is reduced to around 65% and the Voc to around 563 mV at the highest peak firing temperature. Therefore the further degradation of the Ni samples is only explainable by in-diffusion of Ni. But it seems that this effect is saturated after a certain time at a set peak firing temperature equal or over 600°C. Depending on the used belt speed the temperature on the cell is lower than the set peak temperature and lies between 520 and 560°C. It could be that we see the effect of the change between substitutional diffusion at low temperatures and interstitial diffusion at high temperatures (> 600°C set peak temperature). The substitutional diffusion, by substitution of Si atoms in the lattice, is very slow and starts at low temperatures, while the diffusion over interstitials in the Si lattice is very fast ($D \sim 1\ 10^{-6}$ cm^2/s at around 600°C) [10]. Figure 10 shows the diffusion length of nickel in dependency of the temperature for different diffusion times. Below the set peak temperature of 600°C the nickel diffuses by substitutional diffusion into the emitter but not further. Above this temperature the nickel diffuses by interstitial diffusion through the emitter into the silicon bulk reducing the lifetime of the charge carriers and hence reducing pFF and V_{oc}.

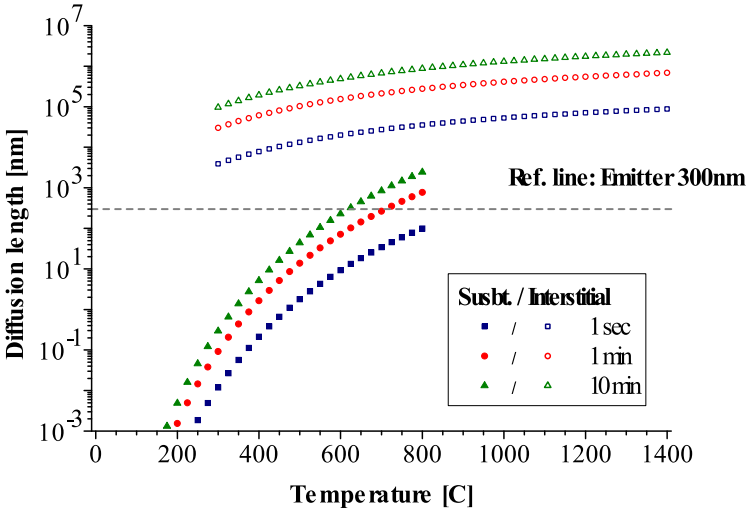

Fig. 10: Diffusion length in dependency of the temperature from the theory of evaporated nickel layers on intrinsic silicon. [10]

4.2. Zinc

Contact formation between the cell and the Zn bulk takes place even through a SiN antireflection layer. But the used glass is too reactive and etches the Si surface strongly resulting in an emitter damage and hence reduction of the V_{oc}. A stronger pFF reduction with increasing firing temperature as for the silver paste samples takes place, which probably means that the emitter is contaminated by in-diffusion of foreign atoms. Crystallite formation takes place but due to the high Pb content their conductivity is quite low resulting in a high contact resistivity. This kind of Pb precipitation via liquid lead was reported by Hong et al. [11], testing glass frits alone on Si and SiN samples. Therefore it is suggested that the Zn in the paste reacts with PbO in the glass frit forming liquid lead:

$$Zn + PbO_{glass} \rightarrow ZnO_{glass} + Pb_{liquid} \qquad (1)$$

The resulting liquid pure lead recrystallises on the [111] planes of the inverted pyramids together with some Zn resulting in crystallites with high Pb content. The amount of Zn compared to the amount of PbO in the paste is quite high so that with reaction 1 not all Zn is oxidized.

The firing in air ambient leads to an oxidization and carbonization on the surface of the zinc particles ($Zn_5(OH)_6(CO_3)_2$). Therefore these particles will not get liquid which means that no sintering takes place. The contact and the adhesion between these particles is very poor (see Fig. 11 a)). Contrariwise during firing under N_2 atmosphere there is no O_2 and CO_2 present which could lead to an oxidization and carbonization. Only lead oxide in the glass frit could oxidize the zinc after equation 1, because lead is a more noble metal than zinc. But the amount of PbO in the paste is very low compared to the amount of zinc, which means that this reaction should be negligible. The sintering of the particles takes place during the firing and only during cooling the surface of the particles gets oxidized and carbonized. Therefore the contact and the adhesion between the particles are better, as Fig. 11 b) schematically shows. If the sample is fired at high temperatures (> 700°C) the liquid melt gets less viscous and starts to wet the whole surface of the sample resulting in a matt SiN surface and rainbow structures around the busbars.

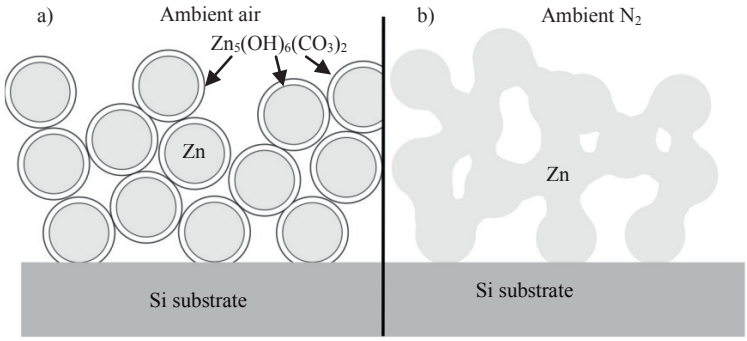

Fig. 11: Schematic drawing of the contact formation and the sintering between the Zn particles a) under air and b) under N_2 atmosphere.

5. Conclusion

With the formulations of the pastes used in this work containing alternative metals it was not possible to create an adequate cheap alternative to Ag screen printing paste. It is possible that the used rudimental glass system does not fit the characteristics of Ni or Zn. However, changes in the paste composition might be promising, e.g. using totally different glass systems, testing various metal particles sizes and shapes. Finally, the Ag/Pb-glass system's simultaneous fire-through/contact formation/sintering functionality within the same temperature window and without degrading the Si bulk may also be quite unique.

Acknowledgements

The research leading to these results has received funding from the Seventh Framework Programme under grant agreement n°228513 (HiperSol).

References

[1] ITRPV-Roadmap; 2013
[2] Yoshida M, Tokuhisa H, Itoh U, Sumita I, Sekine S, Kamata T. Glass-fritless Cu alloy pastes for silicon solar cells requiring low temperature sintering. Proceedings of the 26th EUPVSEC. Hamburg. Germany; 2011. p. 858-860
[3] Bartsch J. Advanced front side metallization for crystalline silicon solar cells with electrochemical techniques. phd thesis. University of Freiburg. ISBN: 978-3-8439-0292-2; 2011
[4] Tous L, Lerat JF, Emeraud T, Negru R, Huet K, Russell R, John J, Poortmans J, Mertens R. Progress in nickel silicide formation using excimer laser thermal annealing. Proceedings of the 27th EUPVSEC. Frankfurt. Germany; 2012. p. 691-695
[5] Butler KT, Vullum PE, Muggerud AM, Cabrera E, Harding JH. Structural and electronic properties of silver/silicon interfaces and implications for solar cell performance. Phys. Rev. B 83(23). 235307. ISSN: 1098-0121; 2011
[6] Løvvik OM, Johnsen SG, Svensson AM, Olibet S, Hoonstra J, Weeber A. Modelling of contacting - from atomistic to macroscopic scale. Talk at ACPV workshop in Oslo. Norway; 2012
[7] Nguyen A, Rane-Fondacaro MV, Efstathiadis H, Haldar P, Michaelson L, Wang C, Munoz K, Tyson T, Gallegos A. Formation of low ohmic contact nickel silicide layer on textured silicon wafers using electroless nickel plating. Proceedings of the 25th EUPVSEC. Valencia. Spain; 2010. p. 2672-2675
[8] Weber ER. Transition metals in silicon. Appl. Phys. A30(1). Doi: 10.1007/BF00617708; 1983. p. 1-22
[9] Kuchling H. Taschenbuch der Physisk. ISBN: 3871440973. Ed. 1; 1979
[10] Alemán M, Bay N, Rudolph D, Rublack T, Glunz SW. Front-side metallization beyond silver paste: Silicide formation / alternative technologies. 1st Metallization Workshop. Utrecht. The Netherlands; 2008
[11] Hong K-K, Cho S-B, You JS, Jeong J-W, Bea S-M, Huh J-Y. Mechanism for the formation of Ag crystallites in the Ag thick-film contacts of crystalline Si solar cells. Solar Energy Materials & Solar Cells 93. DOI: 10.1016/j.solmat.2008.10.021; 2009. p. 898-904